The Seybold Report

ISSN 1533-9211

DOI 10.17605/OSF.IO/F69NU

SPATIAL PATTERN OF LAND USE / LAND COVER CHANGE USING GOOGLE EARTH ENGINE: MAJALENGKA REGENCY 2011-2021

ADRIAN[1], WIDIATMAKA[2], KHURSATUL MUNIBAH[2], IRMAN FIRMANSYAH[3] and ADRIAN[4]

[1]Graduate School of Natural Resources and Environmental Management Science, IPB University. IPB Dramaga Campus, Bogor, West Java, Indonesia.
[2]Department of Soil Science and Land Resource, Faculty of Agriculture, IPB University.
[3]System Dynamics Center.
[4]Departement of Education Geography, Islamic University 45 Bekasi.

Abstract

Physical development requires land, such as the agricultural, housing, industrial, mining, and transportation sectors. The increase in population will undoubtedly increase the need for food and cause changes in Land Use Land Cover (LULC) due to increased land requirements. Majalengka Regency is part of the development of the Rebana Triangle Area (Cirebon-Patimban-Kertajati), which has been planned and designated as a special economic zone (SEZ). This study analyses LULC changes in Majalengka Regency (2011-2021) using Sentinel 2A image data obtained from Google Earth Engine (GEE) for ten years. The LULC classification uses machine learning with a random forest approach combined with NDBI analysis, NDWI and raw rice field maps to produce land cover maps. The image processing results that make land use maps using the smile-Random Forest algorithm on the GEE platform combined with NDWI and NDBI analysis have accurate land cover maps with OA values of 98.81% and kappa 95.91%. The decrease in the area of agricultural land (paddy fields, fields) in Majalengka Regency has decreased by 4457.36 ha in a period of ten years (2011-2021).

Keywords: Google Earth Engine, Land Use Changes, Special Economic Zone Rebana, Paddy Field

INTRODUCTION

Satellite imagery is a vital data source of information for producing land use maps and analyzing temporal maps. (Kempler & Mathews, 2017; Yang et al., 2017). Optical remote sensing data, such as Sentinel, Modis and Landsat ect, are the most prevalent and are frequently employed to analyze land cover change (LULC). Landsat 8 and Sentinel-2's emergence of a new generation of multispectral sensors enables multi-temporal analysis of locations with frequent cloud cover. (Kumar et al., 2016; Mutanga & Kumar, 2019).

In general, users must download satellite data through a data portal, process the data using standalone software, and send the data to end users to process satellite images. With the development of the Google Earth Engine (GEE), processing satellite data on online and cloud-based platforms is now even faster. (Gorelick et al., 2017). The emergence of the GEE cloud platform facilitates the resolution of how remote sensing users can efficiently select data of interest from a vast quantity of remote sensing data. GEE contains multi-source databases, high-performance computing capabilities, online application programming interfaces, and a network-based interactive development environment for developers, enabling robust simulation and computation output. (Amani et al., 2020). Processing with Google Earth Engine

The Seybold Report
ISSN 1533-9211
DOI 10.17605/OSF.IO/F69NU

(GEE). Image data is available in the cloud environment so that users cannot download and upload spatial data.

This research is motivated by the fact that the agricultural sector continues to play a vital role in the development of welfare and the economy for the people of Majalengka Regency, where the agricultural sector's GRDP income is still the highest order (Adrian et al., 2022; BPS, 2018). The most important natural resources required for development are available to land for housing, industry, mining, transportation and the agricultural sector. Agricultural land is a field of land that is used for agricultural business; the availability of agricultural land is very necessary because the increasing population causes food needs also to increase (Gomiero, 2016). Referring to Law of the Republic of Indonesia Number 41 of 2009 on the Protection of Sustainable Food Agricultural Land (LP2B), the lack of potential agricultural land or the reduction of agricultural land will have catastrophic effects on food sovereignty (Perlindungan Lahan Pertanian Pangan Berkelanjutan, 2009).

The uncontrolled expansion of urban areas due to the phenomenon of urbanization can have a negative impact on agricultural land (Gandharum et al., 2022). Lowland agricultural land is highly vulnerable to change into other forms of land use (Adrian et al., 2022; Somantri et al., 2021; Widiatmaka et al., 2014). West Java's Majalengka Regency has vast agricultural land potential and is in this situation. Majalengka Regency, on the other hand, is included in the development of the Rebana Triangle Area (Cirebon-Patimban-Kertajati), which has been planned and designated as a Special Economic Zone (SEZ)(Bappenas, 2018). Thus has the potential for significant changes in agricultural land to non-agriculture that will occur in the Majalengka District.

According to research (Kushardono, 2017; Paramasatya & Rudiarto, 2020), there has been a change in land use in Majalengka as a result of the construction of the West Java International Airport (BIJB) infrastructure, which is part of the Rebana SEZ; The area of the West Java International airport in 2013 was 10.10 Ha and increased to 546.70 Ha in 2018. Thus has the potential for significant changes in agricultural land to non-agriculture that will occur in the Majalengka District. This causes the rice field area to experience a conversion of 413.30 Ha. Thus, the Rebana SEZ area in Majalengka Regency is assumed to have a negative physical impact on the shift in land use, primarily agricultural land on a large scale. Therefore, the purpose of this paper is to find out the spatial pattern of changes in paddy field land cover to built-up land using the Google Earth Engine (GEE) cloud platform so that it can become sustainable spatial information in Majalengka Regency.

MATERIALS AND METHODS

Study area

Majalengka Regency in West Java Province is where the research will take place. Majalengka Regency, which consists of 26 Districts, is geographically situated at coordinates between 108°03' and 108°25' East Longitude and 6°36' and 6°58' South Latitude. Majalengka Regency shares borders with Indramayu Regency to the north, Garut, Tasikmalaya, and Ciamis

The Seybold Report
ISSN 1533-9211
DOI 10.17605/OSF.IO/F69NU

Regencies to the south, Sumedang Regencies to the west, and Cirebon and Kuningan Regencies to the east, the study area could be shown on **Figure 1**

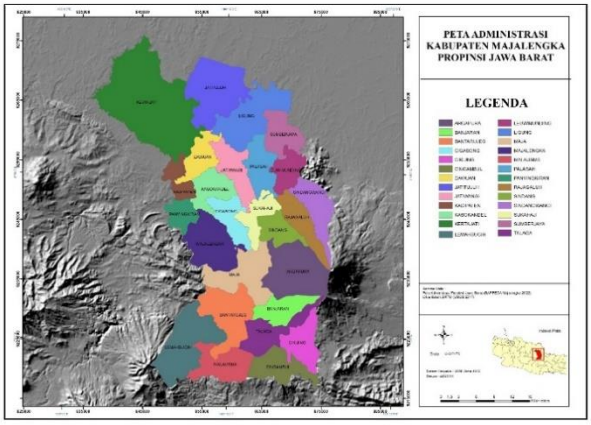

Figure 1: Map of the Study Area of Majalengka Regency.

The research Variables

Some of the data used are primary and secondary data; the primary data that is applied is survey results in the form of checking image interpretation in the field. The secondary data consists of land use maps from 2011 and administrative and rice field standard maps. In addition, satellite imagery is utilized and processed with Google Earth Engine to generate a land use map (GEE) application software (https://code.earthengine.google.com) and ArcMap 10.8. The resulting maps include land use maps for 2011, 2016 and 2021. The data is then confirmed with regional planning data and the Majalengka Regency Spatial Planning for 2011-2031 sourced from the Majalengka Regency Bappeda. In general, the types of data, data sources, data collection techniques, analysis methods and expected outputs could be shown on Table 1:

Table 1: Generated map and sources of original data

No	Year	Data Type	Source	Analysis Techniques	Research Outputs
1	2011	Landuse map	Bappeda	Land cover classification analysis (Supervised) into 9 classes Google Earth Engine Coding and Calibration with CSRT Random Forest Analysis	Spatial pattern of paddy field conversion
2	2021	Administration map	Bappeda		
3	2022	Spatial plan map	Bappeda		
4	2016	Sentinel 2A image	GEE		
5	2021	Sentinel 2A image	GEE		
6	2019	Paddy field distribution map	BPN		

Procedures and data analysis

The research focuses on changing the use of paddy fields in the Majalengka Regency. The stages of land use/cover analysis carried out are; (1) Composing a mosaic of Sentinel-2 MSI (MultiSpectral Instrument) Level-1C and Level-2A image data by combining several scenes with an analysis tool filter date within one year, by including the Sentinel Level-2A collection property orthorectified atmospherically corrected surface reflectance; (2) Take the average

ISSN 1533-9211

DOI 10.17605/OSF.IO/F69NU

(median) value of the image mosaic in that period; (3) Process and cutting image mosaics using the administrative boundary polygons of the research area; (4) Displays image visualization; (5) Determine land use/cover sampling (6) Conduct supervised classification analysis using the Smile-Random Forest machine learning approach; (7) Test and calculate Overall Accuracy (OA) and Kappa Accuracy; (8) Adding NDBI and NDWI analysis to increase accuracy (9) downloading analysis results (10) processing land cover/use maps in ArcGIS to calculate spatial patterns of land change. The land use classification flowchart is presented in Figure 2 below.

Figure 2: **Research Flow Spatial Pattern of Paddy Field Conversion**

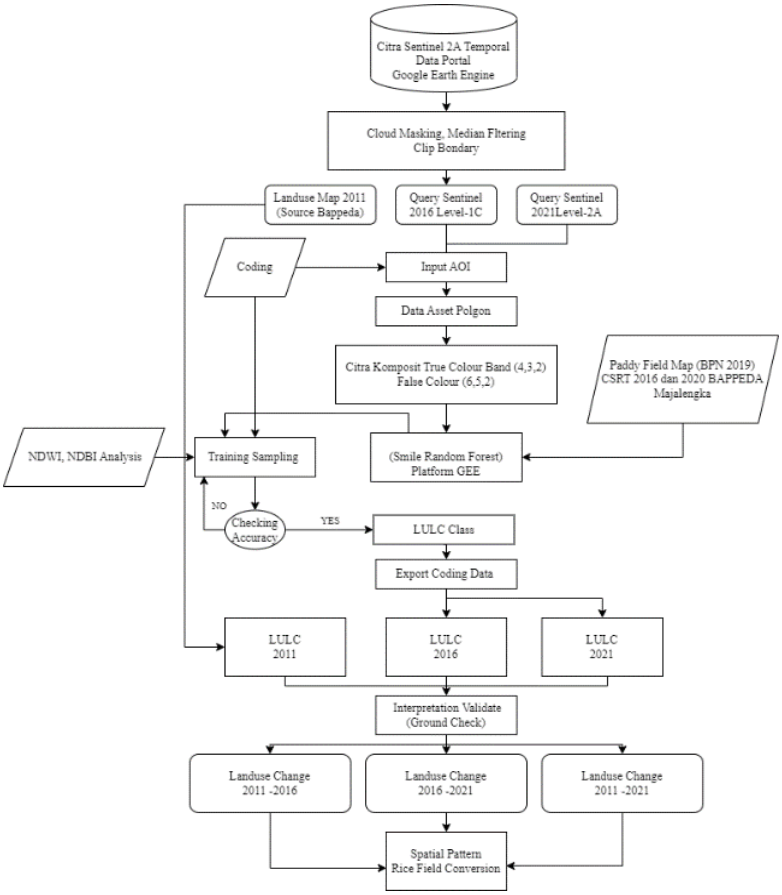

The mapping procedure

The classification of land use/land cover in this research is summarized based on SNI 7645-2014 regulations regarding the classification of land cover and land use. This aggregation results in a classification of 9 land use classes. The 2021 land use/land cover validation test follows the remote sensing procedure using the stratified random sampling estimation method (Sutanto, 1987). The land use/land cover 2021 classification accuracy test uses 400 test points using the stratified random sampling distribution method. Sample points are obtained using the Slovin formula approach based on the number of pixels resulting from the classification, as

The Seybold Report
ISSN 1533-9211
DOI 10.17605/OSF.IO/F69NU

shown in the table above. The google earth engine script to calculate the annual change in land use/land cover in the 2016 and 2021 periods.

a. LULC Classification Methods

Breiman proposed the Random Forest machine learning method (Biau, 2012), a classifier based on a decision tree in which each tree contributes one vote and the final classification or prediction results are determined by voting (Silveira et al., 2019). The RF classification algorithm was implemented on the GEE platform. Training data were utilized for training the RF classifier, whereas verification data were used to assess classification error. Two parameters must be specified when utilizing the RF models in GEE: the number of decision trees to construct per class (number of trees) and the minimal size of a terminal (min leaf). Various values of the number of trees and min-leaves were utilized during the LULC classification. The optimal parameters were determined based on the overall classification precision.google earth engine script for calculating the annual change in cover/usage in the 2016 and 2021 periods is attached in Figure 3.

Figure 3: Random Forest Script Google Earth Engine

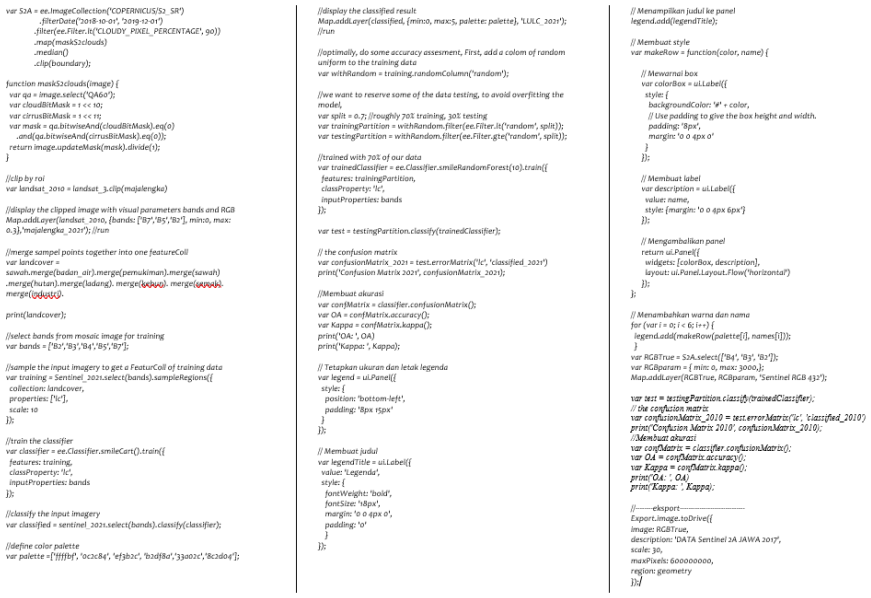

```
var S2A = ee.ImageCollection('COPERNICUS/S2_SR')
            .filterDate('2018-10-01', '2019-12-01')
            .filter(ee.Filter.lt('CLOUDY_PIXEL_PERCENTAGE', 90))
            .map(maskS2clouds)
            .median()
            .clip(boundary);

function maskS2clouds(image) {
 var qa = image.select('QA60');
 var cloudBitMask = 1 << 10;
 var cirrusBitMask = 1 << 11;
 var mask = qa.bitwiseAnd(cloudBitMask).eq(0)
     .and(qa.bitwiseAnd(cirrusBitMask).eq(0));
 return image.updateMask(mask).divide(1);
}

//clip by roi
var landsat_2010 = landsat_3.clip(majalengka)

//display the clipped image with visual parameters bands and RGB
Map.addLayer(landsat_2010, {bands: ['B7','B5','B2'], min:0, max:
0.3},'majalengka_2021'); //run

//merge sampel points together into one featureColl
var landcover =
sawah.merge(badan_air).merge(pemukiman).merge(sawah)
.merge(hutan).merge(ladang). merge(bdbud). merge(awah).
merge(bdbud);

print(landcover);

//select bands from mosaic image for training
var bands = ['B2','B3','B4','B5','B7'];

//sample the input imagery to get a FeatureColl of training data
var training = Sentinel_2021.select(bands).sampleRegions({
 collection: landcover,
 properties: ['lc'],
 scale: 10
});

//train the classifier
var classifier = ee.Classifier.smileCart().train({
 features: training,
 classProperty: 'lc',
 inputProperties: bands
});

//classify the input imagery
var classified = sentinel_2021.select(bands).classify(classifier);

//define color palette
var palette =['ffffbf', '0c2c84', 'ef3b2c', 'b2df8a','33a02c','8c2d04'];
```

```
//display the classified result
Map.addLayer(classified, {min:0, max:5, palette: palette}, 'LULC_2021');
//run

//optimally, do some accuracy assesment, First, add a colom of random
uniform to the training data
var withRandom = training.randomColumn('random');

//we want to reserve some of the data testing, to avoid overfitting the
model,
var split = 0.7; //roughly 70% training, 30% testing
var trainingPartition = withRandom.filter(ee.Filter.lt('random', split));
var testingPartition = withRandom.filter(ee.Filter.gte('random', split));

//trained with 70% of our data
var trainedClassifier = ee.Classifier.smileRandomForest(10).train({
 features: trainingPartition,
 classProperty: 'lc',
 inputProperties: bands
});

var test = testingPartition.classify(trainedClassifier);

// the confusion matrix
var confusionMatrix_2021 = test.errorMatrix('lc', 'classified_2021')
print('Confusion Matrix 2021', confusionMatrix_2021);

//Membuat akurasi
var confMatrix = classifier.confusionMatrix();
var OA = confMatrix.accuracy();
var Kappa = confMatrix.kappa();
print('OA:', OA)
print('Kappa: ', Kappa);

// Tetapkan ukuran dan letak legenda
var legend = ui.Panel({
 style: {
  position: 'bottom-left',
  padding: '8px 15px'
 }
});

// Membuat judul
var legendTitle = ui.Label({
 value: 'Legenda',
 style: {
  fontWeight: 'bold',
  fontSize: '18px',
  margin: '0 0 4px 0',
  padding: '0'
  }
});
```

```
// Menampilkan judul ke panel
legend.add(legendTitle);

// Membuat style
var makeRow = function(color, name) {

    // Mewarnai box
    var colorBox = ui.Label({
     style: {
      backgroundColor: '#' + color,
      // Use padding to give the box height and width.
      padding: '8px',
      margin: '0 0 4px 0'
      }
    });

    // Membuat label
    var description = ui.Label({
     value: name,
     style: {margin: '0 0 4px 6px'}
    });

    // Mengamballikan panel
    return ui.Panel({
     widgets: [colorBox, description],
     layout: ui.Panel.Layout.Flow('horizontal')
    });
};

// Menambahkan warna dan nama
for (var i = 0; i < 6; i++) {
 legend.add(makeRow(palette[i], names[i]));
 }
var RGBTrue = S2A.select(['B4', 'B3', 'B2']);
var RGBparam = { min: 0, max: 3000,};
Map.addLayer(RGBTrue, RGBparam, 'Sentinel RGB 432');

var test = testingPartition.classify(trainedClassifier);
// the confusion matrix
var confusionMatrix_2010 = test.errorMatrix('lc', 'classified_2010')
print('Confusion Matrix 2010', confusionMatrix_2010);
//Membuat akurasi
var confMatrix = classifier.confusionMatrix();
var OA = confMatrix.accuracy();
var Kappa = confMatrix.kappa();
print('OA: ', OA)
print('Kappa: ', Kappa);

//------eksport-----------------------
Export.image.toDrive({
image: RGBTrue,
description: 'DATA Sentinel 2A JAWA 2017',
scale: 30,
maxPixels: 600000000,
region: geometry
})
```

b. Algorithm of NDBI

Normalized Difference Built-up Index (NDBI) is an algorithmic approach used to estimate the level of built-up areas (Vigneshwaran & Vasantha Kumar, 2018). The principle of this algorithm approach is to sharpen building objects to the ratio value between midi-infrared (MIR) and near-infrared (NIR) bands. Based on its characteristics, objects in the built area reflect a higher MIR band than the NIR band. In some cases, dry land and built-up areas have the same pattern and characteristics where the MIR reflectance value is much higher than that of NIR waves (Gao, 1996). The formula for calculating NDBI can be seen in Table 2 (Gómez

ISSN 1533-9211

DOI 10.17605/OSF.IO/F69NU

et al., 2020). The commonly used index is the Normalized Difference Built-up Index, also known as the NDBI. NDBI is widely used in mapping analysis of the existence of built-up areas using remote sensing imagery. This algorithm can increase the accuracy of built-up land for residential land cover.

c. Algorithm of NDWI

The Normalized Difference Water Index (NDWI) is a method for identifying water objects. Because water objects have high reflectance characteristics in the green spectrum (GREEN) and high absorption rates in the near-infrared spectrum, the algorithm employs green and infrared bands (RED). By comparing the values of the two bands, the radiometric value of objects containing water will be greater than that of other objects. (Gao, 1996; Sellars et al., 2013). When NDWI extracts more water bodies in the context of structures, such as water bodies in cities, the extracted water body information deviates significantly from the actual water body information. By adding this algorithm, it can increase the accuracy of land cover for water bodies and agricultural land. The formula for calculating NDWI can be seen in Table 2; the flow of merging the NDBI and NDWI platforms with land cover/use classification can be seen in figure 4.

Table 2: Spectral Index Formula

No.	Indeks	Formula
1	NDBI	NDVI = (NIR - RED) / (NIR + RED)
2	NDWI	NDWI = (NIR - SWIR) / (NIR + SWIR1)

Figure 4: Combining NDBI, NDWI Methods with Land Cover Analysis

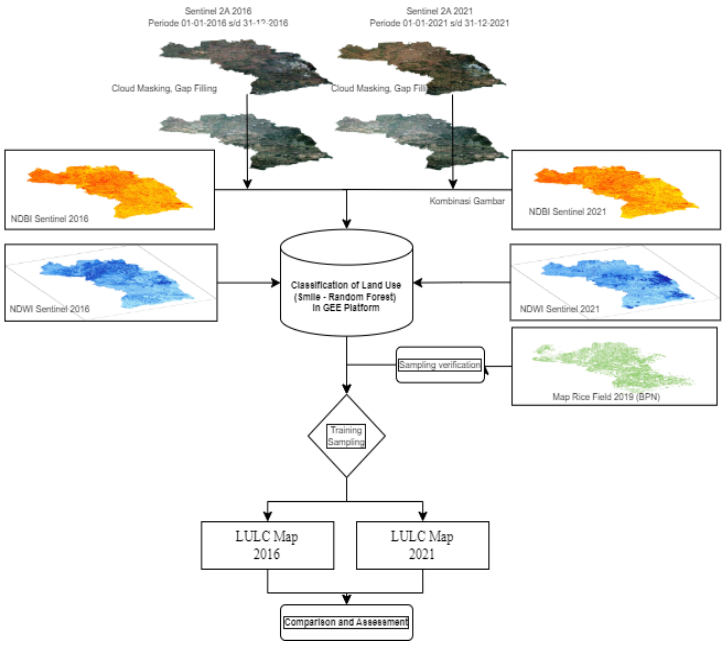

The Seybold Report
ISSN 1533-9211
DOI 10.17605/OSF.IO/F69NU

d. Interpretation and Calculation of Maping Procedure

The validation used is the field data verification approach and sample point tests at study locations. In testing the accuracy of this step, follow the approach and assessment method of stratified random sampling for remote sensing (Sutanto, 1987) as follows:

1. Field inspection at a number of selected sampling points for each type of land use, where for paddy fields a deeper inspection is carried out. Each type of land cover/use is associated with a number of sampling areas based on the homogeneity of the sampling points.
2. Comparing the suitability of the results of image classification analysis with actual field conditions
3. The results of the analysis of digital image data are carried out by calculating the matrix (confusion matrix) for the type of land cover/use where the level of accuracy will be known. Sampling points are obtained using the Solvin formula (Roziqin & Kusumawati, 2017).

$$\mathbf{D = s/s(a)^2 + 1}$$

Where:

D = sample;

s = population;

a = 90% precision value or sig. = 0.1

d. Primary survey or site verification

Formulating land cover/land use results data on existing field conditions are needed, for it requires validation of the existing 2021 land use which obtained with a field survey approach. The primary survey or site verification involves direct monitoring of the study area and taking documentation of field conditions related to land use to verify existing land use and sample sizes for each type of land use, as shown in Table 3.

Table 3: Validation of Land Use / Land Cover Samples (Ground Truth)

Land use / Land cover (SNI 7645-2014)	Cell count (10x10) m	Number of Samples
1. Paddy field	4826671	145
2. Field	3140747	94
3. Mixed Crop	3023493	91
4. Scrub	28748	1
5. Forest	365871	11
6. Settlement	1689374	51
7. Water body	144720	4
8. Industrial Area	33457	1
9. Airport	71652	2
Total	13324733	400

ISSN 1533-9211

DOI 10.17605/OSF.IO/F69NU

RESULTS

Land use accuracy

The confusion matrix was used to determine the land cover/use classification analysis findings; table 4 displays the user's and producer's total accuracy as determined by the confusion matrix data. The percentage of pixels that are correctly categorized in terms of land use is known as overall accuracy; overall accuracy is the percentage of pixels that are correctly classified in terms of land use, While the user's accuracy reveals the error in classifying the pixels in the incorrect category of land use, the producer's accuracy reveals the accuracy of the pixels classified in different categories (Duan et al., 2019).

Formulating a land cover/use change prediction requires data on existing field conditions (Halmy et al., 2015). Validation of existing land use is carried out in 2021 obtained from 2020 spot image data combined with field survey results in 2022. The sampling population for this study was obtained from the number of cells on the 2021 land use map, while the sampling with a precision value of 90% was seen from the ability of the researchers seen from the need for time, human resources and the area of the observation area (Arikunto, 2010). The rice field raw land map used as an independent variable is made in raster format. In producing an accurate map, vector data is converted into a raster format with a spatial resolution of 10 m. This spatial resolution corresponds to Sentinel 2A imagery, which has the exact resolution. The percentage accuracy of land use/land cover classification is calculated by comparing the appropriate sample to the number of samples proven in the field; the results of calculating the accuracy of each land use type are explained.

Table 4: Land use accuracy results

		Field survey Validation											
		1	**2**	**3**	**4**	**5**	**6**	**7**	**8**	**9**	**Total**	**Not Suitable**	**Suitable**
LU/LC Clasification	**1**	142	3								145	3	97,93%
	2		90	2	2						94	4	95,74%
	3	1	3	87							91	4	95,60%
	4				1						1	-	100,00%
	5					11					11	-	100,00%
	6						51				51	-	100,00%
	7							4			4	-	100,00%
	8								1		1	-	100,00%
	9									**2**	2	-	100,00%
Total											**400**	**11**	**98,81%**

LU/LC	1. Paddy field	4. Scrub	7. Water body
Code	2. Field	5. Forest	8. Industry
	3. Mixed Crop	6. Settlement	9. Airport

The confusion matrix calculation and the Kappa coefficient value were used to analyze the accuracy of trial data. This accuracy test was conducted to determine the best outcomes for each machine learning algorithm used (Google Earth Engine) and the output of the findings of

The Seybold Report
ISSN 1533-9211
DOI 10.17605/OSF.IO/F69NU

the mapping of land cover and land use. Comparing the classification outcome classes with the classes used in the training data on image sampling, when confusion matrix is one way to assess the overall accuracy value of calculation results and classification processing.

Land use with the highest user accuracy was achieved in 2016 and 2021 in the bush, forest, settlement, water bodies, and industry and airport classes with 100% results. The lowest user accuracy in 2016 was field land at 90.32%; in 2021, it was 93.62%. The accuracy of paddy fields in 2016 was 96.55%, while in 2021, combined with field surveys, it had an accuracy of 97.24%. Due to their rotational cropping practices, this discrepancy resulted from farmers' frequent conversion of fields in the study region to paddy fields. Overall accuracy can demonstrate that the RF used in the GEE platform provides a reliable model for mapping land use at two-time points, namely 2016 and 2021, with a range of 97.81% to 98.81%, with a relatively low level of misclassification. The minimum accuracy for land cover/land use maps is 85%, according to research by (Rana & Venkata Suryanarayana, 2020); so the findings of this study are reasonably accurate as input for the following analysis process.

Table 5: Land use accuracy results 2016 and 2021

Land use / Land cover	2016		2021	
	Users's Accuracy	Producer's Accuracy	Users's Accuracy	Producer's Accuracy
1. Paddy field	98,62	96,55	97,93	97,24
2. Field	97,87	90,32	95,74	93,62
3. Mixed Crop	96,70	93,48	95,6	95,6
4. Scrub	100	100	100	100
5. Fores	100	100	100	100
6. Settlement	100	100	100	100
7. Water body	100	100	100	100
8. Industrial Area	100	100	100	100
9. Airport	100	100	100	100
Overall accuracy	99,24%	97,81	98,81	98,49

According to research findings (Gandharum et al., 2022; Piao et al., 2021; Singha et al., 2019), using RF on the GEE platform can generate highly accurate maps, with OA reaching 92.6%. The results of this study found agreement with those findings. This research's findings align with those of other studies showing that combining images and indexes can improve classification curation over using just one classification's results (Carrasco et al., 2019). When combined with corrections to the raw rice field map derived from BPN (Badan Pertanahan Nasional) data, NDBI and NDWI analyses of the land cover map on the GEE platform produce excellent accuracy on the land cover classification analysis. This results in an accurate land cover for agricultural land, especially using paddy fields. Below are descriptions of the outcomes of the data processing and data processing that result in land use images.

ISSN 1533-9211

DOI 10.17605/OSF.IO/F69NU

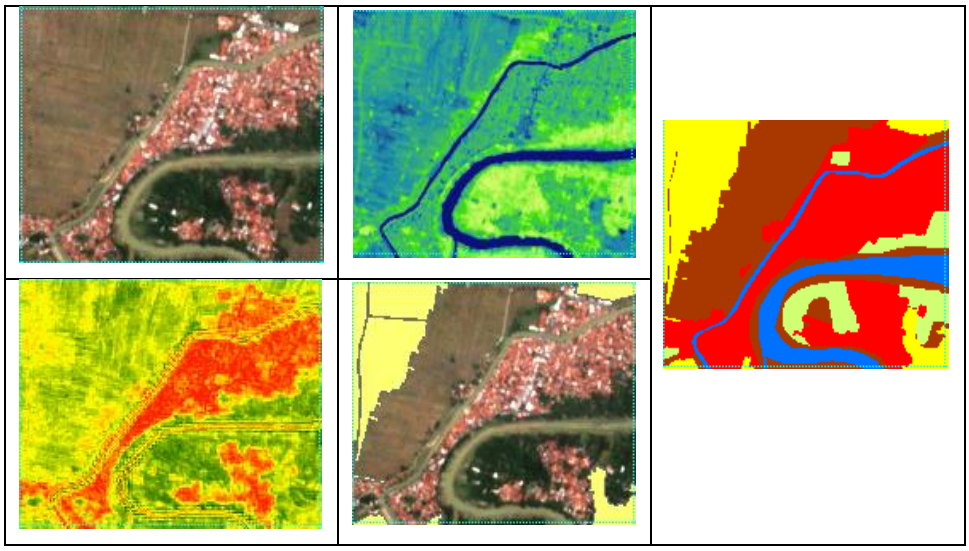

Figure 5: Comparison of Index Predictor Variables: Sentinel Imagery, NDWI, NDBI, and Paddy Field Map

Results of land use / land cover period 2011 – 2016 and 2016 – 2021

The validated land use and cover data for Majalengka Regency for 2011, 2016, and 2021 were then calculated for each land use and cover area category and overlapped (overlaid) between the three time periods. GIS is used for map overlay so that it is possible to track changes in land use. Statistical calculations of shifts in land cover/use reveal the dynamics of current land use. The classification results of Sentinel 2A imagery from 2016 and 2021 were used to calculate changes in land use and cover over the two different classification results' respective periods.

The land use that was examined covers the land cover and use in 2011 and 2016 as well as in 2021. Based on the analysis's findings and calculations, it is possible to determine the area of land use in 2011, 2016, and 2021. This spatial analysis sought to determine the distribution of items in industrial areas, settlements, and changes in the area of each paddy field's use during that time. Calculations of land cover/use change are used to categorize and quantify the various degrees and magnitudes of land change. The findings below show the area and percentage of land use changes in the year's three seasons.

The Seybold Report
ISSN 1533-9211
DOI 10.17605/OSF.IO/F69NU

Table 6: Comparison of Land Use Area in years (2011, 2016 and 2021)

Penggunaan Lahan	2011 (Ha)	%	2016 (Ha)	%	L 2021 (Ha)	%
1. Paddy field	59.899,62	33,23	59.450,63	32,98	58.339,46	32,36
2. Field	46.993,92	26,07	46.527,01	25,81	44.096,72	24,46
3. Mixed Crop	45.104,24	25,02	44.957,62	24,94	43.183,78	23,95
4. Scrub	1.537,67	0,85	1.537,67	0,85	1.537,67	0,85
5. Fores	8.917,99	4,95	8.917,99	4,95	8.917,96	4,95
6. Settlement	13.561,73	7,52	14.072,77	7,81	18.951,46	10,51
7. Water body	2.247,76	1,25	2.247,45	1,25	2.182,44	1,21
8. Industrial Area	9,66	0,01	82,07	0,05	346,60	0,19
9. Airport	-	-	479,39	0,27	716,49	0,40
Total	178.272,60	100	178.272,60	100	178.272,60	100

Land use in Majalengka Regency in 2011, 2016, and 2021 when viewed from its use. Most of it is paddy fields; based on the results of the analysis above, it is known that the spatial dynamics of land cover/use in Majalengka Regency. Each type of existing land use has changed, namely the addition of area or reduction of land use area. A decrease in the area of paddy fields dominates changes in land use/cover. Paddy fields experienced a significant decrease during 2016 – 2021, amounting to 1560.17 Ha.

Followed by a decrease in agricultural land by 2897.19 ha and the area of mixed crop by 1920.47 ha; an increase followed the decrease in agricultural land in the area of other land uses during that period. The increase in land use includes the area covered/used by residential, airport and industrial land during 2016 – 2021. Residential land use is calculated to have an area of 14,072.77 Ha, while in 2021, residential land use will increase to 18,951.46 Ha. Industrial land use in 2016 was 82.07 Ha, while in 2021, it will be 346.60 Ha. Land use for airport facilities (BIJB) has increased in area by 479.39 Ha in 2016 and will continue to increase to 716.49 Ha in 2021. The land use in 2011, 2016 and 2021 is described in the following map.

Figure 6: **Map of Land Use Change in Majalengka Regency**

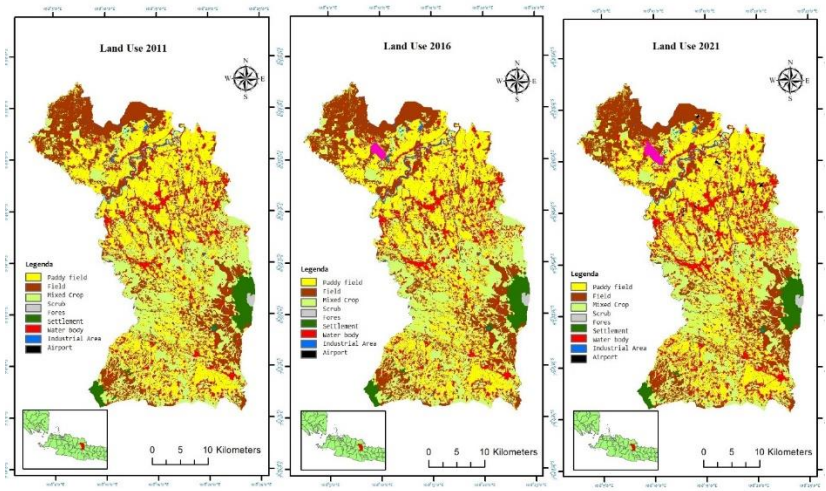

The Seybold Report
ISSN 1533-9211
DOI 10.17605/OSF.IO/F69NU

Changes in land cover/use were analyzed using ArcGIS software. This analysis uses an overlay technique approach and table matrix calculations to obtain changes in each land use type. Land use maps for 2011, 2016 and 2021 were used to analyze changes in land use in the 2011-2016 and 2016-2021 periods. Furthermore, the 2011 land cover/use map was stacked with the 2016 land use map to analyze and obtain changes in land use in the 2011 – 2016 period. After the two period cover/use change maps for 2011 – 2016 and 2016 – 2021 are obtained, these two maps are overlaid to obtain land use changes in 2011 – 2021; for the calculation of the land change matrix can be explained in the table below.

Table 7: Land Use/Land Cover Change Matrix

		LU/LC 2021									
		1	2	3	4	5	6	7	8	9	Total
LU/LC 2011	1	58.339,46					999,89		185,7	374,58	59.899,63
	2		44.096,72				2586,96		69,21	241,02	46.993,91
	3			43.183,78			1818,41		41,84	60,22	45.104,25
	4				1.537,67						1.537,67
	5					8.917,96	0,02				8.917,98
	6						13.520,01		39,52	2,2	13.561,73
	7							2.182,44	0,68	38,46	2.247,76
	8								9,66		9,66
	9									716,48	716,48
		1.560,17	2.897,19	1.920,47	0	0,02	41,72	65,32	336,95	716,48	178.272,60

LU/LC	1. Paddy field	4. Scrub	7. Water body
Code	2. Field	5. Forest	8. Industry
	3. Mixed Crop	6. Settlement	9. Airport

After obtaining the results from the analysis of land cover/use changes, calculate the conversion matrix of land use changes (Land Use/Land Cover Changes Conversion Matrix). The spatial distribution of changes in land use area accompanied by validation with field data is shown in the following figure.

Paddy Field Becomes Built-up Land for the 2011–2021 Period

Transfer of functions related to land conversion is a dynamic and continuous process that will occur in line with population developments or regional development patterns. Conversion in paddy fields will occur more often than in other agricultural lands because paddy fields are generally located in relatively strategic areas. The results of the calculations and analysis show that land change is dominated by the transition of agricultural land where paddy fields become settlements, or fields become settlements, and mixed gardens become residential land. From a spatial perspective, the most significant change in paddy field land into settlements occurred in Majalengka District, the capital and centre of government, namely 83.96 ha in 10 years. The next position occurred in Kertajati District, which was 62.33 ha due to the transfer of the function of the airport development. When viewed spatially, changes in agricultural land into settlements occurred in the Kertajati sub-district of 248.76 ha due to the conversion of the function of the airport development. The third position is in the Sumberjaya District, with an area of 144.48 ha, an industrial area that correlates with residential areas.

ISSN 1533-9211

DOI 10.17605/OSF.IO/F69NU

There are indications of an increasing need for residential land in Majalengka Regency, which has become the centre of industrial growth and the impact of establishing the Rebana Special Economic Zone (Rebana SEZ). This change accommodates the housing needs of industrial workers who need land for settlements. Based on the analysis and field survey results, there has been a significant increase in land use to become industrial land. Changes in the cover/use of paddy fields into industrial land which experienced an increase of 181.11 Ha; farmland into industrial land use of 61.69 Ha and mixed crop into industrial land use of 41.34 Ha, the distribution area of industry as seen from the results above is more spread in the northern and central areas of Majalengka Regency; The spatial distribution of land change is presented in the figure below.

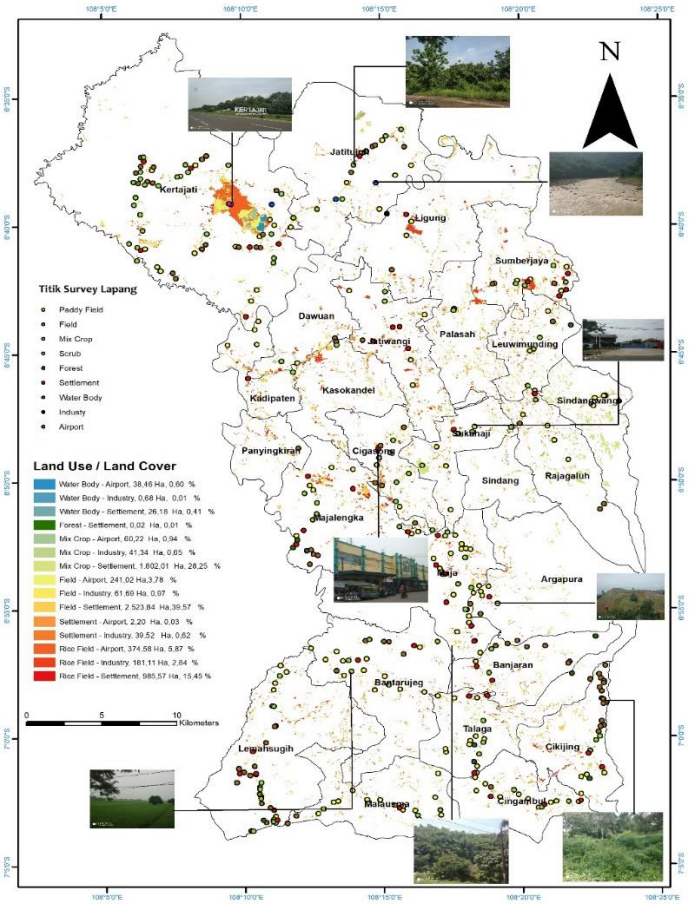

Figure 7: Map of Spatial Pattern Changes (Field Validation)

DISCUSSION

The results of the facts on the ground that changes in agricultural land cover/use conditions in Majalengka Regency, namely West Java International Airport (BIJB) Kertajati and its surroundings, have changed due to development, which is dominant in the administrative area

ISSN 1533-9211

DOI 10.17605/OSF.IO/F69NU

of Kertajati District. For the construction of the airport, agricultural land has changed due to land conversion covering an area of 374.58 ha for paddy fields, 241.02 ha for fields and 60.22 ha for mixed garden land has been converted to runways. And the development of the airport area. The development and expansion of the BIJB area have the potential to generate impacts, both positive and negative impacts occur, in the community around the airport location. The negative impact that occurs due to the conversion of agricultural land where there will be a reduction in the production of agricultural commodities, especially rice which is a staple food.

With the conversion of agricultural land that occurs, the production capacity of agricultural commodities will decrease or even disappear. Land conversion also has implications for reducing job opportunities for farmers in rural areas in Majalengka Regency, which is the top source of GRDP income for Majalengka Regency and various agricultural infrastructure (investments) that have been built. Land conversion and change of function is a dynamic process that will always occur, which follows the development of the population and the pattern of development of an area. In densely populated areas (urban) in Majalengka Regency as well as in suburban areas (suburban), land conversion follows the direction of development that occurs where land use has a high economic value, such as economic facilities and infrastructure such as factories, settlements, shopping centres, Special economic zones and others. For areas with a minimal population (rural), the development pattern that focuses on the agricultural sector actually tends to the conversion of agricultural land, especially the use of paddy fields. Conversion to the use of paddy fields often occurs in comparison. Generally, it occurs more dominantly in other agricultural lands due to the location of paddy fields with high productivity and fertility rates, which are generally located in strategic areas.

CONCLUSION

Results of this study show that land use classification using the smile-Random Forest algorithm on the GEE platform combined with NDWI and NDBI analysis produces an accurate land cover map with an OA value of 98.81% and a kappa of 95.91%. The area of agricultural land (rice fields, fields) in Majalengka Regency has decreased by 4457.36 ha in ten years (2011-2021). It is necessary to carry out future planning efforts/strategies to anticipate massive changes in agricultural land in Majalengka Regency. This study also concluded that land use classification using the smile-Random Forest algorithm on the GEE platform could produce highly accurate maps, which is >98% and can shorten the process and analysis time. Therefore, the classification of paddy field use using RF on the GEE platform can be a platform for periodic mapping of paddy field use in the Majalengka Regency and other areas.

Acknowledgements

The authors would like to salute the Majalengka Regional Government and its stakeholders. They have taken the time and contributed to the discussion in determining decisions regarding the importance of this research's driving factors. This investigation was supported by LPDP (Indonesia Endowment Funds for Education).

ISSN 1533-9211

DOI 10.17605/OSF.IO/F69NU

References

1) Adrian, Widiatmaka, Munibah, K., & Firmansyah, I. (2022). Evaluate land suitability analysis for rice cultivation using a GIS-based AHP multi-criteria decision-making approach: Majalengka Regency, West Java Province. IOP Conference Series: Earth and Environmental Science, 1109(1), 012062. https://doi.org/10.1088/1755-1315/1109/1/012062

2) Amani, M., Ghorbanian, A., Ahmadi, S. A., Kakooei, M., Moghimi, A., Mirmazloumi, S. M., Moghaddam, S. H. A., Mahdavi, S., Ghahremanloo, M., Parsian, S., Wu, Q., & Brisco, B. (2020). Google Earth Engine Cloud Computing Platform for Remote Sensing Big Data Applications: A Comprehensive Review. IEEE Journal of Selected Topics in Applied Earth Observations and Remote Sensing, 13. https://doi.org/10.1109/JSTARS.2020.3021052

3) Arikunto. (2010). Teknik Sampel. In Prosedur Penelitian Suatu Pendekatan Praktik-Revisi ke X.

4) Bappenas. (2018). Pedoman Pelaksanaan Intervensi Penurunan Stunting Terintegrasi di Kabupaten/Kota. Rencana Aksi Nasional Dalam Rangka Penurunan Stunting: Rembuk Stunting.

5) Biau, G. (2012). Analysis of a random forests model. In Journal of Machine Learning Research (Vol. 13, pp. 1063–1095).

6) BPS. (2018). Kabupaten Majalengka dalam angka tahun 2018. In BPS Kabupaten Majalengka. Badan Pusat Statistik.

7) Duan, Q., Tan, M., Guo, Y., Wang, X., & Xin, L. (2019). Understanding the spatial distribution of urban forests in China using Sentinel-2 images with Google Earth Engine. Forests, 10(9). https://doi.org/10.3390/f10090729

8) Gandharum, L., Hartono, D. M., Karsidi, A., & Ahmad, M. (2022). Monitoring Urban Expansion and Loss of Agriculture on the North Coast of West Java Province, Indonesia, Using Google Earth Engine and Intensity Analysis. Scientific World Journal, 2022(Sdg 2). https://doi.org/10.1155/2022/3123788

9) Gao, B. C. (1996). NDWI - A normalized difference water index for remote sensing of vegetation liquid water from space. Remote Sensing of Environment, 58(3), 257–266. https://doi.org/10.1016/S0034-4257(96)00067-3

10) Gómez, J. A., Patiño, J. E., Duque, J. C., & Passos, S. (2020). Spatiotemporal modeling of urban growth using machine learning. Remote Sensing, 12(1). https://doi.org/10.3390/rs12010109

11) Gomiero, T. (2016). Soil degradation, land scarcity and food security: Reviewing a complex challenge. In Sustainability (Switzerland) (Vol. 8, Issue 3). https://doi.org/10.3390/su8030281

12) Gorelick, N., Hancher, M., Dixon, M., Ilyushchenko, S., Thau, D., & Moore, R. (2017). Google Earth Engine: Planetary-scale geospatial analysis for everyone. Remote Sensing of Environment, 202, 18–27. https://doi.org/10.1016/j.rse.2017.06.031

13) Halmy, M. W. A., Gessler, P. E., Hicke, J. A., & Salem, B. B. (2015). Land use/land cover change detection and prediction in the north-western coastal desert of Egypt using Markov-CA. Applied Geography, 63, 101–112. https://doi.org/10.1016/j.apgeog.2015.06.015

14) Kempler, S., & Mathews, T. (2017). Earth science data analytics: Definitions, techniques and skills. Data Science Journal. https://doi.org/10.5334/dsj-2017-006

15) Kumar, P., Pandey, P. C., Singh, B. K., Katiyar, S., Mandal, V. P., Rani, M., Tomar, V., & Patairiya, S. (2016). Estimation of accumulated soil organic carbon stock in tropical forest using geospatial strategy. Egyptian Journal of Remote Sensing and Space Science, 19(1), 109–123. https://doi.org/10.1016/j.ejrs.2015.12.003

16) Kushardono, D. (2017). Klasifikasi Penutup/Penggunaan Lahan Dengan Data Satelit Penginderaan Jauh

The Seybold Report
ISSN 1533-9211
DOI 10.17605/OSF.IO/F69NU

Hiperspektral (Hyperion) Menggunakan Metode Neural Network Tiruan. Jurnal Penginderaan Jauh Dan Pengolahan Data Citra Digital, 13(2). https://doi.org/10.30536/j.pjpdcd.2016.v13.a2516

17) Mutanga, O., & Kumar, L. (2019). Google earth engine applications. In Remote Sensing (Vol. 11, Issue 5). https://doi.org/10.3390/rs11050591

18) Paramasatya, A., & Rudiarto, I. (2020). Implikasi Penetapan Wilayah Pusat Pertumbuhan Industri Terhadap Penggunaan Lahan Di Kabupaten Majalengka. Jurnal Pembangunan Wilayah & Kota, 16(2), 144–157. https://doi.org/10.14710/pwk.v16i2.22257

19) Piao, Y., Jeong, S., Park, S., & Lee, D. (2021). Analysis of land use and land cover change using time-series data and random forest in north korea. Remote Sensing, 13(17). https://doi.org/10.3390/rs13173501

20) Rana, V. K., & Venkata Suryanarayana, T. M. (2020). Performance evaluation of MLE, RF and SVM classification algorithms for watershed scale land use/land cover mapping using sentinel 2 bands. Remote Sensing Applications: Society and Environment, 19. https://doi.org/10.1016/j.rsase.2020.100351

21) Roziqin, A., & Kusumawati, I. (2017). Analisis Pola Permukiman Menggunakan Data Penginderaan Jauh di Pulau Batam. IRONS: 8th Industrial Research Workshop and National Seminar Politeknik Negeri Bandung, 52–58.

22) Sellars, S., Nguyen, P., Chu, W., Gao, X., Hsu, K. L., & Sorooshian, S. (2013). Computational earth science: Big data transformed into insight. Eos (United States). https://doi.org/10.1002/2013EO320001

23) Silveira, E. M. O., Silva, S. H. G., Acerbi-Junior, F. W., Carvalho, M. C., Carvalho, L. M. T., Scolforo, J. R. S., & Wulder, M. A. (2019). Object-based random forest modelling of aboveground forest biomass outperforms a pixel-based approach in a heterogeneous and mountain tropical environment. International Journal of Applied Earth Observation and Geoinformation, 78, 175–188. https://doi.org/10.1016/j.jag.2019.02.004

24) Singha, M., Dong, J., Zhang, G., & Xiao, X. (2019). High resolution paddy rice maps in cloud-prone Bangladesh and Northeast India using Sentinel-1 data. Scientific Data, 6(1). https://doi.org/10.1038/s41597-019-0036-3

25) Somantri, L., Ridwana, R., & Himayah, S. (2021). Land value analysis in the suburban of Bandung and agricultural land availability impact. IOP Conference Series: Earth and Environmental Science, 683(1). https://doi.org/10.1088/1755-1315/683/1/012088

26) Sutanto. (1987). Prinsip dasar penginderaan jauh. In Panduan Aplikasi Penginderaan Jauh Tingkat Dasar.

27) Perlindungan Lahan Pertanian Pangan Berkelanjutan, Pub. L. No. No. 41 Tahun 2009, 2009 31 (2009).

28) Vigneshwaran, S., & Vasantha Kumar, S. (2018). Extraction of built-up area using high resolution Sentinel-2A and Google satellite imagery. International Archives of the Photogrammetry, Remote Sensing and Spatial Information Sciences - ISPRS Archives, 42(4/W9), 165–169. https://doi.org/10.5194/isprs-archives-XLII-4-W9-165-2018

29) Widiatmaka, W., Ambarwulan, W., Firmansyah, I., Munibah, K., Santoso, P. B. K., & Sudarsono, S. (2014). Land suitability and dynamic system modelling to define priority areas of soybean plantation in paddy fields in Karawang, West Java. Agrivita, 36(3), 235–248. https://doi.org/10.17503/Agrivita-2014-36-3-235-248

30) Yang, C., Huang, Q., Li, Z., Liu, K., & Hu, F. (2017). Big Data and cloud computing: innovation opportunities and challenges. In International Journal of Digital Earth (Vol. 10, Issue 1, pp. 13–53). https://doi.org/10.1080/17538947.2016.1239771